proceedings

MDPI

*Proceedings*

# MgO-Doped (Zr,Sr)$TiO_3$ Perovskite Humidity Sensors: Microstructural Effects on Water Permeation †

**Hamid Farahani [1,2,*], Rahman Wagiran [3] and Gerald Urban [1,2]**

[1] Freiburg Materials Research Centre, FMF, University of Freiburg, Stefan-Meier-Str. 21, 79104 Freiburg, Germany; urban@imtek.de
[2] Laboratory for Sensors, Department of Microsystems Engineering, IMTEK, University of Freiburg, Georges-Koehler-Allee 103, 79110 Freiburg, Germany
[3] Department of Electrical and Electronic Engineering, Faculty of Engineering, University Putra Malaysia, UPM, Serdang, Selangor 43400, Malaysia; rwagiran@upm.edu.my
* Correspondence: hamid.farahani@imtek.de; Tel.: +49-761-203-4771
† Presented at the Eurosensors 2017 Conference, Paris, France, 3–6 September 2017.

Published: 8 August 2017

**Abstract:** Porous $(Zr_{0.5},Sr_{0.5})TiO_3$ and MgO (1, 3, 5 mol%) doped ZST nanocomposites have been developed and investigated as humidity sensing elements. The surface area analyser and FESEM data have indicated that the MgO doped perovskites are contained of the macropores and grain size of about 77 to 87 nm. EFTEM proved the reduction of particle size by addition of MgO dopant concentration. While pure ZST shows BET surface area of about 58 $m^2/g$, MgO doped samples exhibit about 12 $m^2/g$. Sensor contained of ZST doped with 3 mol% MgO shows highest sensitivity with about four orders of magnitude change in impedance within the range of 20% to 95% RH.

**Keywords:** humidity sensors; perovskite materials; thick film; nanocomposites; ceramic; zirconium

## 1. Introduction

The monitoring of ambient humidity, especially in the compound form with different gases by accurate, high efficient, low power and provident sensors are gained attention of many application fields [1]. Measurement and control of environmental relative humidity play an important role in today's life [2]. Hygrometers are classified on the basis of transduction technologies, sensing materials, and mechanisms. Based on our previous comprehensive survey on the humidity sensors, nowadays RH sensors are assorted to organic, inorganic, organic/inorganic, and carbon types [3].

Humidity sensors' performance are strongly depend on the microstructure and morphology of the sensing medium or film [4]. In case of thin/thick film humidity sensors, the desirable characteristics whose improve sensitivity are determined by such properties including high porosity, large specific surface area, proper pore size distribution and higher conductivity of the ions [5]. Although humidity sensors are produced from different materials, most of them apply a same sensing principle which is the occurrence in surface of substance and capillary condensation of vapor inside the pores. Basic of the moisture sensing is physical and chemical adsorption of water molecules [6]. Ceramic type humidity sensors based on metal oxides have exhibited some superior advantages in comparison to polymer films from the viewpoints of their mechanical strength, thermal capability, physical stability and their resistance to chemical attack, which reveals them to be the most promising materials for chemical humidity sensor applications [3]. However, ceramic matters themselves vulnerable to insufficient superficial conductivity at low humidity, therefore signal drift. As far as ionic conduction is strongly dependent on the formation of monolayer and multilayer by physisorption and capillary condensation of the water vapour molecules, therefore perovskites'

humidity sensing characteristics largely depend on the film complex microstructures, such as surface area, effective porosity, volume and pore size distribution [3]. In this communicate we have reported the design and fabrication of thick film humidity sensors based on various perovskite-based ZST nanocomposites synthesized through solid state reaction. The transduction mechanism of the sensors has also been discussed.

## 2. Materials and Methods

### *2.1. Chemicals*

Zirconium(IV) carbonate ≥40% $ZrO_2$ basis ($Zr(OH)_2CO_3 \cdot ZrO_2$), strontium carbonate ≥99.9% trace metal basis ($SrCO_3$), titanium(IV) oxide ≥99% ($TiO_2$), and magnesium oxide nanopowder <50 nm particle size (BET) MgO all from Sigma Aldrich, were used as precursors. Butyl carbitol acetate 2-(2-Butoxyethoxy)ethyl acetate ≥99.2%, alpha-terpineol ($C_{10}H_{18}O$) and ethyl alcohol all from Sigma Aldrich were used as solvents. Ethyl cellulose (48% ethoxyl) from Sigma Aldrich was used as resin.

### *2.2. Materials Synthesis and Doping*

Humidity sensitive powders were synthesized through solid state reaction method from $SrCO_3$, $Zr_3CO_8$, and $TiO_2$ precursors. Equimolar amount of basic powders were weighted and mixed based on molar ratio. To having homogenous slurry mixture, powders ultrasonically bathed for 24 h utilizing ultrasonic water bath. The compounds were wet milled for 8 h using acetone as grinding medium by adopting planetary mono mill. Then ball ground slurry was dried at 50 °C overnight and intermediate ground to fine powder using mortar and pestle. Solid state reaction has taken place by calcination of ground compounds inside the horizontal tubular furnace at 1000 °C in air atmosphere for 3 h. A homogenous nanocomposite of $(Zr_{0.5},Sr_{0.5})TiO_3$ was obtained and stored for further characterizations. To have nanocomposites with different doping values MgO used as doping agent and as-received (particle size < 50 nm). 1, 3 and 5 mol% of magnesium oxide were added to certain proper values of $(Zr,Sr)TiO_3$ and $(1 - x)(Zr_{0.5},Sr_{0.5})TiO_3$-$(x)MgO$ (x = 0.01, 0.03, 0.05) nanocomposites were prepared through SSR method following the above described procedure.

### *2.3. Sensors Fabrication and Characterization*

The experiments were performed with four different types of nanocomposites i.e., $(Zr_{0.5},Sr_{0.5})TiO_3$ (hereafter ZST) and ZST doped with 1, 3, and 5 mol% MgO (hereafter ZSTM1, ZSTM3, and ZSTM5) as active layers. Organic vehicle was prepared by mixing and stirring of alpha-terpineol, ethyl cellulose, and butyl carbitol with 12:1:12 ratio. Printing inks were prepared by admixture of fine nanocomposite powders and organic compounds in ratio of 73:27. Conducting gold electrodes with 7 pairs of interdigitated fingers have been printed by means of automat screen printing machine then subjected to drying process and followed by firing at 1000 °C inside the microwave furnace. As last layer, sensing elements transferred onto an alumina substrate and coated substrates were placed in UV-belt dryer at temperature of 150 °C for 15 min. Dried films were annealed inside of the box furnace at 1100 °C for half an hour to form active layers. Micro humidity sensors were wire bonded by the Molex male wafer 5pins connector to be able for experimental test setups. Humidity sensing properties of the manufactured sensors were evaluated under the laboratory-made setup conditions (temperature-gas-humidity controlled chamber) at continuous range of 20% to 95% RH. The AC electrical humidity characteristics and electrochemical impedance spectroscopy (EIS) were carried out by means of computer controlled 4294A precision impedance analyzer (20 Hz–2 MHz). The measurement was conducted via 4 wire type Kelvin clip lead connection (two-point probe). The DC electrical resistance of the prototypes was measured via four-point probe method (keithley) at 25 °C.

## 3. Results and Discussion

### *3.1. SEM Characterization*

Surface morphology of the cured ceramic sensors were determined by means of Field Emission Scanning Electron Microscopy (FESEM) and illustrated in Figure 1a–d. The micrographs revel that grains are grown by additive surcharges. Homogenous distribution of dopant nanoparticles are seen. All the films are well developed with sufficient degree of porosity. By increment of magnesia dopants the grains size had matured with slight decrease of porosity. The most porous body can be seen in Figure 1a as pure ZST and follows by ZST doped with different MgO concentrations in Figure 1b–d, respectively. The MgO nanoparticles (size of about smaller than 40 nm) were added to ZST as surface conductivity-enhanced agents and there was an expectation to atomic reduction of open cavities. Average grain size of the samples can be found in Table 1.

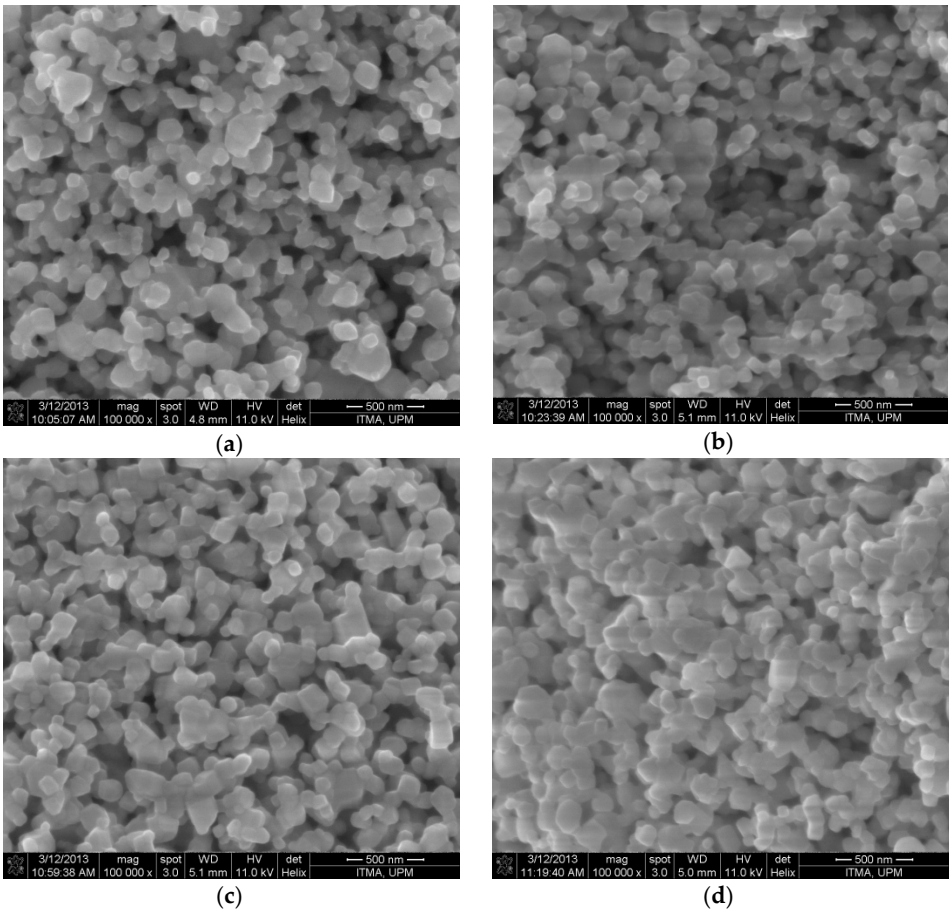


**Figure 1.** FESEM micro-photograph of four types of sensors annealed at 1100 °C: (**a**) ZST; (**b**) ZST doped 1 mol% MgO; (**c**) ZST doped 3 mol% MgO; (**d**) ZST doped 5 mol% MgO.

### *3.2. Microstructural Properties*

Energy Filtered Transmission Electron Microscopy (EFTEM) applied on as-calcined nanopowders to observe average particle size, particles morphology, and influence of doping agents. Specific surface area and total volume of the pores were then measured from output data of Surface Area (Porosity) Analyzer unit based on $N_2$ gas sorption. The specific surface area and pore radius were determined by multi point BET and BJH theory from adsorption and desorption isotherm by 11 and 13 data points, respectively. While pure ZST contains of mesoporosity, samples contained of magnesia dopants exhibit macroporosity. Detailed specifications of the nanocomposites lists in Table 1.

**Table 1.** Surface area, pore radius, average particle size and grain size of the nanocomposites and thick film sensors as function of the doping value.

| Specimen | Surface Area ($m^2/g$) | Pore Radius (nm) | Particle Size (nm) | Grain Size (nm) |
|---|---|---|---|---|
| ZST | 58 | 1.72 | 40.3 | 69 |
| ZST-MgO (1 mol%) | 11 | 97.22 | 32.9 | 77 |
| ZST-MgO (3 mol%) | 11.6 | 99.38 | 34.4 | 81 |
| ZST-MgO (5 mol%) | 11.76 | 110.37 | 36.3 | 87 |

### *3.3. Humidity Sensing Characteristics*

Changes in resistance values of micro humidity sensors versus different humidity levels at room temperature are plotted in Figure 2a. The variations of magnitude of resistance have been fitted by the linear fit lines as drawn in plot. Based on the extracted equations from the plots the extrapolated values of R were estimated. Humidity dependency of the bulk specific electrical conductance for humidity range of 20% to 95% RH at room temperature for the ZST sensor is plotted in Figure 2b. The regressive trend of the resistance plots versus increase of the humidity levels specifies that the prototypes are operating on the basis of ionic conduction mechanism which occours through proton-hopping therefore strong polarization of water electrolytes. In agreement with morphological microstructures this transduction is caused by water vapour physisorption, multilayer formation and then capillary condensation of molecules inside of the capillary pores at surface (proton mobility or charge carriers enhancement). Changes in resistance is very significant for the ZSTM3 and then ZST thick films in the 20% to 95% RH range. The ZST sensor resistance shifts by three orders of magnitude from $9.2E^7$ to $244E^3$ which is acceptable for the provskite-based sensor, while this change is more than four orders of magnitude (from $1.2E^8$ to $81.8E^3$) for the ZSTM3 device. ZSTM1 and ZSTM5 specimens comes only with two orders of magnitude changes from $2.7E^8$ to $6E^6$ and $1.8E^8$ to $3.2E^6$, respectively.

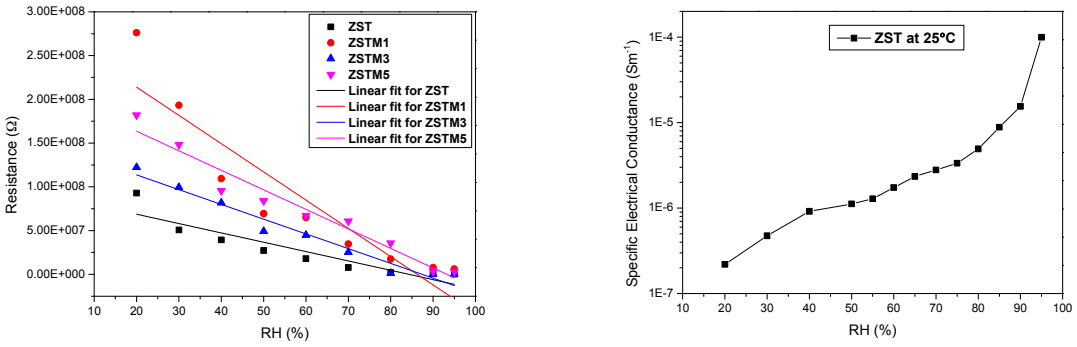


(**a**) (**b**)

**Figure 2.** (**a**) Resistance change of the sensors versus relative humidity of 20% to 95% RH at room temperature fitted with the linear lines; (**b**) humidity dependency of the bulk electrical conductivity for humidity range of 20%–95% RH at room temperature for the ZST micro sensor.

### Sensitivity

In this research the sensitivity is defined as the ratio of the resistance variations ($\Delta R$ between highest and lowest RH values) to the resistance values at lowest RH levels as percentage:

$$S = \frac{R_{Humid} - R_{Dry}}{R_{Dry}} \times 100 \quad (1)$$

$R_H$ and $R_D$ represent the resistance at 95% to 20% RH and resistance at 20% RH, respectively. As shown in Figure 3, all the specimens exhibit logarithmic behaviour in entire RH range with ZSTM3 as most sensitive transducer with 99.94% change.

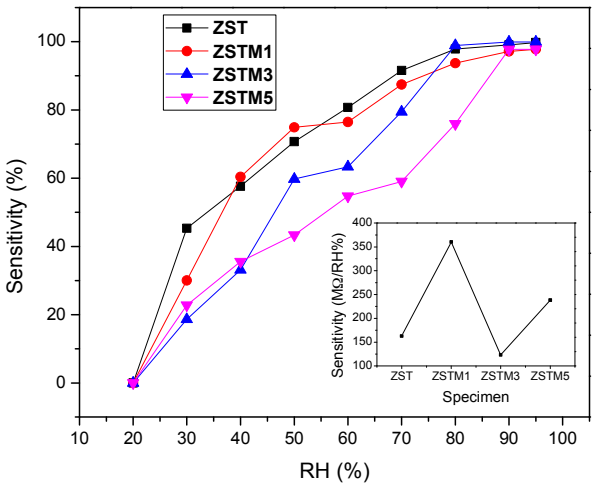


**Figure 3.** Sensitivity comparison between sensors at different humidity levels, and Inset; based on samples at entire RH range (from 20% to 95%).

In summary, we showed that perovskite $(Zr_{0.5},Sr_{0.5})TiO_3$ is a promising candidate for moisture sensing purpose. Structural analysis has proved MgO doping agents are highly influenced on ZST. Decrement of surface area by addition of dopants is due to a low $N_2$ adsorption rate of magnesia. The electrical results are showing that while doping surcharges are influenced on mesoporosity and growth of grains, they act as surface conductivity-enhanced agents.

**Conflicts of Interest:** The authors declare no conflict of interest.

## References

1. Oprea, A.; Courbat, J.; Bârsan, N.; Briand, D.; de Rooij, N.F.; Weimar, U. Temperature, Humidity and Gas Sensors Integrated on Plastic Foil for Low Power Applications. *Sens. Actuators B Chem.* **2009**, *140*, 227–232.
2. Norris, A.; Saafi, M.; Romine, P. Temperature and Moisture Monitoring in Concrete Structures Using Embedded Nanotechnology/microelectromechanical Systems (MEMS) Sensors. *Constr. Build. Mater.* **2008**, *22*, 111–120.
3. Farahani, H.; Wagiran, R.; Hamidon, M.N. Humidity Sensors Principle, Mechanism, and Fabrication Technologies: A Comprehensive Review. *Sensors (Basel)* **2014**, *14*, 7881–7939.
4. Salehi, A.; Nikfarjam, A.; Kalantari, D.J. Highly Sensitive Humidity Sensor Using Pd/Porous GaAs Schottky Contact. *IEEE Sens. J.* **2006**, *6*, 1415–1421.
5. Shah, J.; Kotnala, R.K.; Singh, B.; Kishan, H. Microstructure-Dependent Humidity Sensitivity of Porous $MgFe_2O_4$–$CeO_2$ Ceramic. *Sens. Actuators B Chem.* **2007**, *128*, 306–311.
6. Traversa, E. Ceramic Sensors for Humidity Detection: The State-of-the-Art and Future Developments. *Sens. Actuators B Chem.* **1995**, *23*, 135–156.